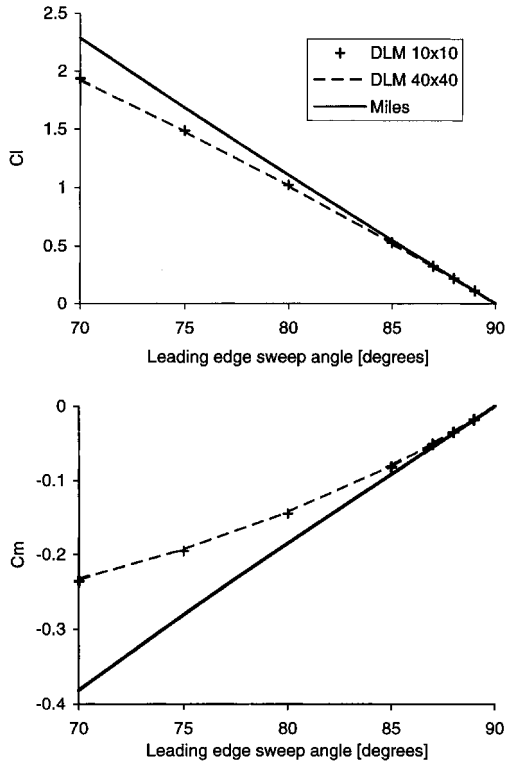

Fig. 4 Comparison with Miles' slender wing theory.[6]

the estimated converged DLM results and the slender wing theory decrease monotonically from 0.4% in C_l and 1% in C_m at 89.5 deg to 0.02% in both C_l and C_m at 89.95 deg. It would therefore seem that the DLM converges to the correct results for slender delta wings in steady flow.

Conclusions

The subsonic DLM is sufficiently robust to give credible solutions for delta wings with root-to-tip paneling schemes, despite the excessive box aspect ratios that usually occur at the tip. The present study suggests that there is no practical upper limit to box aspect ratio, with a box aspect ratio of 291 having been used without encountering any difficulties.

The convergence with respect to simultaneous refinement of equally spaced chordwise and spanwise divisions is approximately linear with respect to $1/\sqrt{n}$. This property is useful for estimating the discretization error of a particular paneling scheme, or for estimating the fully converged solution using extrapolation.

A comparison with slender wing theory indicates that the DLM converges to the correct results for slender delta wings in steady flow.

References

[1]Albano, E., and Rodden, W. P., "A Doublet-Lattice Method for Calculating Lift Distributions on Oscillating Surfaces in Subsonic Flows," *AIAA Journal*, Vol. 7, No. 2, 1969, pp. 279–285.

[2]Rodden, W. P., Giesing, J. P., and Kalman, T. P., "New Developments and Applications of the Subsonic Doublet-Lattice Method for Nonplanar Configurations," CP-80-71, AGARD, Nov. 1970 (Paper 4).

[3]Rodden, W. P., Taylor, P. F., and McIntosh, S. C., Jr., "Further Refinement of the Subsonic Doublet-Lattice Method," *Journal of Aircraft*, Vol. 35, No. 5, 1998, pp. 720–727.

[4]Chen, P. C., Sarhaddi, D., Liu, D. D., Karpel, M., Stritz, A. G., and Jung, S. Y., "A Unified Unsteady Aerodynamic Module for Aeroelastic, Aeroservoelastic and MDO Applications," *Proceedings of the International Forum on Aeroelasticity and Structural Dynamics*, Vol. II, Associazione Italiana di Aeronautica ed Astronautica, Rome, Italy, 1997, pp. 123–139.

[5]Van Zyl, L. H., "Convergence of the Subsonic Doublet Lattice Method," *Journal of Aircraft*, Vol. 35, No. 6, 1998, pp. 977–979.

[6]Miles, J. W., *Potential Theory of Unsteady Supersonic Flow*, Cambridge Univ. Press, London, 1959, pp. 132–134.

Improvement to Numerical Predictions of Aerodynamic Flows Using Experimental Data Assimilation

G. Barakos,* D. Drikakis,† and W. Lefebre‡
University of Manchester, Manchester, England M60 1QD, United Kingdom

I. Introduction

THE idea to use measurements and/or observational data for correcting and updating numerical solutions has already been established in the context of weather forecasting in meteorology.[1–3] In this case, the capability of a numerical forecasting model depends not only on the resolution of the model and the accuracy with which dynamic and physical processes are represented, but it is also dependent critically on the initial conditions employed for integrating the model.

It is known from meteorology that observational data and/or measurements cannot be directly used to initialize a numerical forecast.[1] The data must be modified in a dynamically consistent manner to obtain a suitable data set for model initialization. This process is usually referred to as "data assimilation." Although the data assimilation technique is already established in the context of weather forecasting, an extensive literature survey showed that there is no systematic research regarding such an approach in the area of aerodynamics.

The aim of the present study is to investigate the idea of experimental data assimilation in the context of aerodynamic computations of turbulent compressible flows over airfoils. Therefore, the objectives of the paper are as follows:

1) To present the implementation of the data assimilation approach in conjunction with a compressible and turbulent Navier–Stokes solver.

2) To investigate the effects of pressure and velocity forcing on the numerical prediction of subsonic and transonic flows over an airfoil.

II. Experimental Data Assimilation

The compressible two-dimensional Navier–Stokes equations, in conjunction with a two-equation turbulence model, formed the computational basis for the present study. An implicit-unfactored method,[4] which solves the Navier–Stokes and turbulence transport equations in a strongly coupled fashion, has been employed. The solver uses a first order in time-implicit discretization scheme with Newton-type subiterations and Gauss–Seidel relaxation. A third-order characteristic-based scheme is used for discretizing the inviscid fluxes. The Launder–Sharma (LS)[5] and Nagano-Kim (NK)[6] k-ε models have also been employed. To improve the predictions of the LS model in separated flows, the Yap-correction term[7] has been included in the transport equation for $\tilde{\varepsilon}$.

Experimental data are usually available for surface pressure distributions, and, possibly, for the velocity profiles at certain positions around the geometry. We consider an airfoil for which experimental data for the pressure coefficient distribution C_p on the suction

Received Nov. 1, 1998; revision received Jan. 20, 1999; accepted for publication Jan. 21, 1999.

*Ph.D. Candidate, Institute of Science and Technology, Department of Mechanical Engineering, P.O. Box 88.

†Lecturer, Institute of Science and Technology, Department of Mechanical Engineering, P.O. Box 88; currently Lecturer, Queen Mary and Westfield College, Engineering Department, University of London, London E1 4NS, England, United Kingdom. Member AIAA.

‡M.Sc. Student, Institute of Science and Technology, Department of Mechanical Engineering, P.O. Box 88.

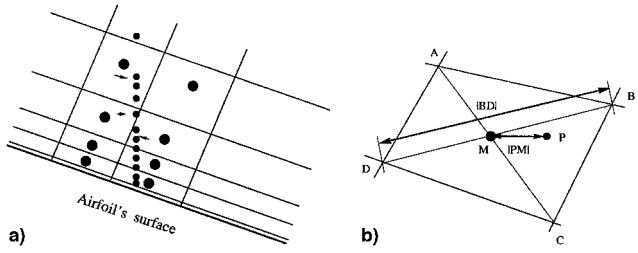

Fig. 1 a) Schematic of the experimental points position on the computational grid, and b) definition of the cell distances used in Eq. (2).

and pressure sides are available. The Navier–Stokes solver requires boundary conditions for the conservative variables. Because the pressure coefficient distribution is provided by the experiment, the total energy at the wall e_w can be calculated by

$$e_w = p_w/(\gamma - 1) \tag{1}$$

also taking into account that the kinetic energy of the fluid and the turbulent kinetic energy vanish on the airfoil's surface.

The positions where measurements have been taken will not, generally, correspond to the grid-points coordinates, and, therefore, an interpolation procedure should be applied. In all calculations presented here, linear interpolation for the pressure has been used.

A second alternative for experimental data assimilation is to force a velocity profile at a certain position of the flowfield. This is not actually consistent with the standard definition of Navier–Stokes's boundary conditions, but its investigation was attempted complementary to the pressure-forcing to examine possible accuracy and stability effects on the Navier–Stokes algorithm. Moreover, it is worth investigating whether by fixing locally few experimental velocity data, the numerical solution elsewhere in the flowfield can be improved. A brief description of the velocity-forcing implementation is given next.

Let us consider a velocity profile that has experimentally been obtained at a certain position over the airfoil. The experimental measurements are schematically shown as small dots in Fig. 1, and these are placed over the computational cells, shown as big dots in the same figure. In the general case, the coordinates of the experimental points do not coincide with the cell centers' coordinates, and, additionally, depending on the grid density, each computational cell may encompass more than one measurement point. This is actually the case for the experimental velocity data used in the present study, apart from the near-wall region in which velocity measurements are usually difficult to be obtained.

The algorithm for the velocity forcing initially searches the computational domain to find all cells in which experimental data exist. Every computational cell in which measurement points are contained will, henceforth, be labeled a "forced cell." Furthermore, for each forced cell, only one measurement value is needed to implement the velocity forcing. One option is to define the forced value u_{force} by properly selecting one of the experimental points contained in the cell. As a distance criterion a weighting coefficient was defined by

$$\beta = |PM|/|BD| \tag{2}$$

The distances $|PM|$ and $|BD|$ are shown in Fig. 1, where M is the cell center and P is the experimental point. According to the preceding criterion, the selected measurement point is the one with the smallest value of β.

No-slip boundary conditions are used for the velocity components at the solid boundary. The density gradient normal to the wall is set equal to zero and the same is done for the total energy gradient, but only in the case of velocity forcing. In the case of pressure forcing, Eq. (1) is used to calculate the total energy at the wall (e_w).

The LS and NK models use the same boundary conditions for the turbulent kinetic energy and dissipation rate at solid boundaries, namely, $k_w = 0$ and $\tilde{\varepsilon}_w = 0$. In the freestream and at the inlet of the computational domain, the turbulent kinetic energy must be specified. In this work, k_∞ was taken as 1% of the kinetic energy of the fluid. The freestream value of the turbulent dissipation rate is determined by fixing the turbulent length scale. In this work ε_∞ was calculated as

$$\varepsilon_\infty = C_\mu^{3/4}\left(k_\infty^{3/2}/l\right)$$

where l was taken to be $\frac{1}{60}$ of a characteristic length of the problem, which here is the chord length of the airfoil c.

III. Results

Implementation and investigation of pressure and velocity forcing were carried out for subsonic and transonic flow cases for which experimental results are available. The first case is the subsonic flow ($M_\infty = 0.15$) around the ONERA–A airfoil[8] at Reynolds number $Re = 2 \times 10^6$ and at angle of incidence $\alpha = 13.3$ deg. A computational grid with 300×80 points was used, and the transition point was fixed at $x/c = 0.05$ on both sides of the airfoil. The second case is the transonic flow ($M_\infty = 0.754$) around the RAE-2822 airfoil[9] at Reynolds number $Re = 6.5 \times 10^6$ and at angle of incidence $\alpha = 2.81$ deg. For this airfoil the grid was 355×70 and the transition point was fixed at $x/c = 0.02$. Experience with low-Re number turbulence models[4] has shown that the preceding grids provide sufficient resolution of the turbulent boundary layer having the first computational node at $y^+ = 0.5$.

In the preceding cases, experimental results for the wall pressure–coefficient distribution, as well as for the velocity and turbulent kinetic energy profiles, at various positions over the airfoil, are available.

A. Pressure Forcing

In Fig. 2, the pressure coefficient distributions for the subsonic and transonic flow cases are shown. In the case of pressure forcing, the C_p values shown in this figure are obtained after interpolating the experimental values on the cell centers.

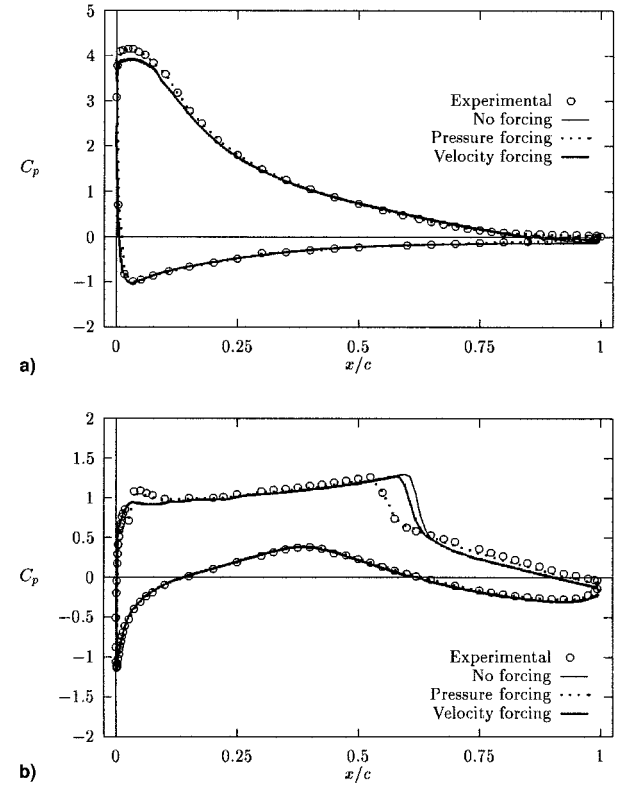

Fig. 2 Wall C_p distributions: a) on the ONERA-A airfoil ($M_\infty = 0.15$, $Re = 2 \times 10^6$, $\alpha = 13.3$ deg), and b) on the RAE-2822 airfoil ($M_\infty = 0.754$, $Re = 6.5 \times 10^6$, $\alpha = 2.81$ deg).

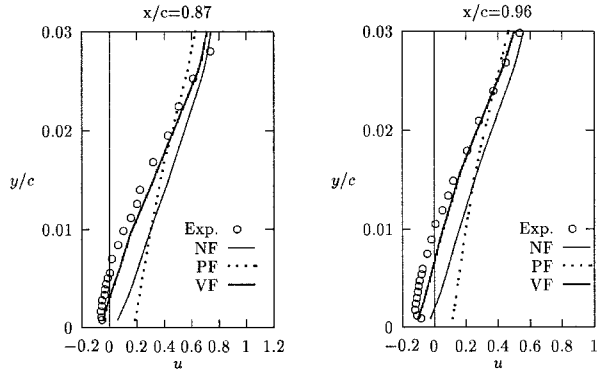

Fig. 3 ***u*-velocity profiles over the ONERA-A airfoil: NF, no forcing; PF, pressure forcing; and VF, velocity forcing.**

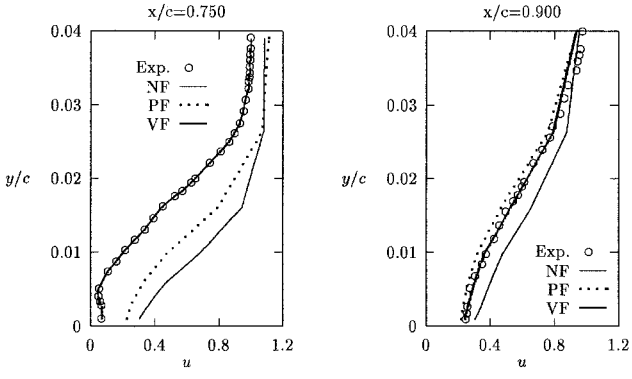

Fig. 4 ***u*-velocity profiles over the RAE-2822 airfoil: NF, no forcing; PF, pressure forcing; and VF, velocity forcing.**

The effects of pressure forcing on the velocity profiles can be seen in Figs. 3 and 4, where the numerical predictions are compared with the experimental data and the unforced numerical solution at two positions. It is pointed out that the numerically obtained velocity profiles have been plotted after interpolating them along the direction of the experimental velocity measurements; i.e., normal to the airfoil's surface. This is why the numerical profiles do not start exactly from the wall but from the same position as the experimental ones.

In the subsonic case, pressure forcing does not improve the numerical solution, particularly in the near-wall region. However, pressure forcing has more important effects on the transonic case and this can be explained as follows: The numerical solution without pressure forcing fails to capture the correct shock position, due to inadequacy of the turbulence model, which mainly leads to a shift of the shock location. By imposing the experimental C_p values as a boundary condition, the shock location is now given to the solver as additional information, and, as a result, the deficiency of the turbulence model is removed and the numerical predictions are significantly improved.

B. Velocity Forcing

For the ONERA case, an experimental velocity profile over the airfoil in the separated flow region, at $x/c = 0.87$, was selected for applying the velocity forcing. Eight experimental points along the profile were selected. Initially, another velocity profile in the wake, at $x/c = 1.2$, was also imposed, and it was found that forcing the wake values does not lead to any improvement of the results. Therefore, we present results using only the velocity profile at $x/c = 0.87$.

For the subsonic case, comparisons between forced and unforced solutions of the pressure-coefficient distribution as well as velocity profiles are shown in Figs. 2a and 3, respectively. In the subsonic case, the velocity forcing does not affect the predictions of the pressure coefficient, and its effect is more significant on the velocity profiles, particularly in the separated flow region ($x/c = 0.96$). The unforced solution cannot capture the extent of the separated flow region, whereas the velocity forcing does a very good job. While the improvement occurs at all positions in the separated flow region, the velocity forcing did not alter significantly the profiles in the wake (plots are not included).

For the transonic flow case, the results using velocity forcing are shown in Figs. 2b and 4 for the C_p and velocity profiles, respectively. Six experimental points were employed to force the u velocity at $x/c = 0.75$. The computations show that velocity forcing slightly improves the pressure-coefficient distribution, but significantly improves the velocity profiles.

In all of the preceding computations, the unforced solution was used to initiate the calculations of pressure and velocity forcing. This was found necessary to avoid numerical stability problems. The additional computational effort to obtain the solution when applying forcing was approximately the one-fifth of the total computational time.

IV. Conclusions

An investigation of experimental data assimilation in turbulent aerodynamic flows was presented. For the subsonic flow, pressure forcing had a marginal to no effect on the numerical prediction, with either turbulence model being used. However, pressure forcing significantly improved the numerical prediction of the transonic flow. Without pressure forcing the shock location was shifted downstream, leading to significant misprediction of the velocity profiles.

Velocity forcing had a positive effect on both subsonic and transonic flow simulations. In the subsonic case, separation of the flow close to the trailing edge occurs and this was very poorly captured by the solution without velocity forcing. However, by forcing the velocity profile in only one position over the airfoil, better predictions in the whole separation region were obtained. In the transonic flow, velocity forcing also improved the predictions. The velocity profiles were better predicted when velocity forcing rather than pressure forcing was used. Both pressure and velocity forcing had no effect on velocity, turbulent kinetic energy and shear-stress profiles in the wake. Moreover, forcing the solution by using a wake velocity profile did not improve the numerical predictions. Finally, pressure forcing is easier to implement into the solver, and it can also be more easily obtained experimentally.

Overall, the experimental data assimilation was found to lead to an improvement of the numerical solution. The need to use experimental data assimilation emerges from the difficulty to develop turbulence models that provide high accuracy in a broad category of flow problems. Turbulence modeling has been characterized as the pacing item in computational fluid dynamics (CFD), and this picture does not seem to change, at least in the near future. Therefore, a closer synergism between CFD and experiment on the basis of experimental data assimilation may be a promising alternative for accurate CFD predictions.

Acknowledgments

D. Drikakis would like to acknowledge the discussions he had with Rob Harrison, Tassos Kokkalis, and John Perry at GKN Westland Helicopters, Ltd., in connection with the idea of imposing experimental values as boundary conditions in aerodynamic flows. The motivation for the present study emerges partly from the encouragement we had from the preceding colleagues regarding the investigation of this approach.

References

[1] Holton, J. R., "An Introduction to Dynamic Meteorology," *International Geophysics Series*, 3rd ed., Vol. 48, Academic, San Diego, CA, 1992.

[2] Ruggiero, F. H., Sashegyi, K. D., Madala, R. V., and Raman, S., "The Use of Surface Observations in Four-Dimensional Data Assimilation Using a Mesoscale Model," *Monthly Weather Review*, Vol. 124, No. 5, 1996, pp. 1018–1033.

[3] Haltiner, G. J., and Williams, R. T., *Numerical Prediction and Dynamic Meteorology*, 2nd ed., Wiley, New York, 1980.

[4] Barakos, G., and Drikakis, D., "Implicit-Unfactored Implementation of Two-Equation Turbulence Models in Compressible Navier–Stokes Methods," *International Journal for Numerical Methods in Fluids*, Vol. 28, No. 1, 1998, pp. 73–94.

[5]Launder, B. E., and Sharma, B. I., "Application of the Energy-Dissipation Model of Turbulence to the Calculation of Flow near a Spinning Disk," *Letters in Heat and Mass Transfer*, Vol. 1, 1974, pp. 131–138.

[6]Nagano, Y., and Kim, C., "A Two-Equation Model for Heat Transport in Wall Turbulent Shear Flows," *Journal of Heat Transfer*, Vol. 110, No. 3, 1988, pp. 583–589.

[7]Yap, C. R., "Turbulent Heat and Momentum Transfer in Recirculating and Impinging Flows," Ph.D. Dissertation, Faculty of Technology, Univ. of Manchester, Manchester, England, UK, 1987.

[8]Piccin, O., and Cassoudensalle, D., "Etude Dans La Soufflerie F1 Des Profiles AS329 et A240," ONERA, PV 73/1685A YG, Toulouse, France, 1987.

[9]Cook, P. H., McDonald, M. A., and Firmin, M. C. P., "Airfoil RAE2822—Pressure Distributions, and Boundary Layer and Wake Measurements," AGARD-AR 138, 1979.

Computational Simulation of the F-22 Aircraft

Eswar Josyula* and Raymond E. Gordnier†
U.S. Air Force Research Laboratory,
Wright–Patterson Air Force Base, Ohio 45433-7913

Introduction

ACCURATE computational fluid dynamic (CFD) studies of a full aircraft must take into account a good strategy for solving the fluid dynamic equations, ease of grid generation, appropriate turbulence model, and computer capabilities to resolve the flowfield. Subsonic flows at high angle of attack are dominated by effects of vortical structures and possible vortex breakdown. Vortex breakdown severely effects the aircraft stability and control and may reduce the operational envelope of high-performance flight. This problem is particularly relevant to twin-tailed fighters where the tails could be immersed in unsteady flow resulting from the bursting of vortices generated upstream, known as tail buffet.

In this Note, a computational simulation has been performed for the complete aircraft configuration of the F-22. The external flowfield about the aircraft at subsonic speeds and high angle of attack (up to 30-deg incidence) is studied. The effect of yaw on the vortex trajectories is also investigated. Important flowfield details such as the location and strength of the vortical structures are studied qualitatively to elucidate the flow physics and demonstrate the capability of the CFD technology. Results are compared with experimental data[1] for validation of the flow solver. More extensive details about the information presented in this note can be found in the Ref. 2.

The governing equations are taken to be the unsteady three-dimensional, compressible, mass-averaged Navier–Stokes equations. A two-equation k-ε turbulence[3] model is used for the present study. The two-equation model is used because an explicit length-scale specification required for an algebraic model can be difficult to determine and ambiguous for complex geometries involving multiple grids. The mass-averaged Navier–Stokes equations are solved using the numerical code, FDL3DI, which is based on the implicit Beam and Warming algorithm[4] and employs a domain decomposition strategy to handle complex geometries.

Results and Discussion

The flow conditions for the numerical simulation are given in Table 1. The Reynolds number was based on the reference length c of the wing root chord of the model. The full-scale length of the root chord is 240 in. All conditions were selected based on the availability of experimental data.[1] The experiment consisted of a wind-tunnel test of a 0.10-scale model without stores. For the purpose of validation, the surface pressure coefficient measured by the experiment was used.

The grids were generated from a CAD source of the original geometry using the GRIDGEN software.[5] The computation departed from the original geometry only with respect to the engine inlet and outlet. In the computation, a freestream inflow condition was specified at the inlet face with the outflow capped. Overlapping grids were constructed for the various components of the F-22 aircraft, viz. nose, fuselage, inlet, wing, and horizontal and vertical tails. All grids except the nose and inlet grids were of H topology, the nose was C-O topology, and the inlet grids were rectangular. The entire mesh system was embedded within a background mesh extending five root chord lengths away from the body in all directions, except the spanwise direction, which extended two root chord lengths. A minimum distance, $\Delta y/c = 4.6 \times 10^{-5}$, was used in the body normal direction, resulting in $y^+ = 10$ at the first y-mesh point above the surface. Here, c, is the reference length of the wing root chord referred to earlier. Solution convergence was assumed for the high-alpha turbulent solutions when the vortex on the downstream of the aircraft did not change between two solutions three characteristic times apart. All turbulent solutions were started from converged laminar solutions. The data processing rate is 2.6×10^{-5} CPU-seconds/step/node for the turbulent computation on a single processor of the Cray T-90 computer.

The comparison of surface pressure on the upper surface for the experiment[1] and computation is shown in Fig. 1 for an angle of attack of 20 deg. Results at 10- and 30-deg angle of attack are found in Ref. 2. Because of calculations having bilateral symmetry, it is possible to show top views of the F-22 aircraft with one side of the symmetry plane showing the experiment and the other side the computation.

The comparison shows good qualitative agreement between the experiment and computation, and trends given by the experiment are captured in the CFD predictions. Comparison of the computational and experimental surface pressures on the forebody are good. Both experiment and computation display a low-pressure footprint

Table 1 Flow conditions and grid details

Mach number	Re_∞	α, deg	β, deg	Number of nodes, $\times 10^6$	Blocks
0.4	4.6×10^6	10	0	1.0	6
0.4	4.6×10^6	20	0	1.0	6
0.4	4.6×10^6	30	0	1.0	6
0.6	4.6×10^6	24	0	2.0	12
0.6	4.6×10^6	24	6	2.0	12

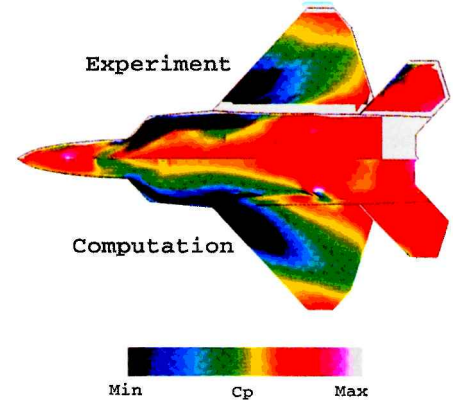

Fig. 1 Top view of comparison of surface pressure. $M_\infty = 0.4$ and $\alpha = 20$ deg.

Presented as Paper 98-0526 at the AIAA 36th Aerospace Sciences Meeting, Reno, NV, Jan. 12–15, 1998; received Aug. 3, 1998; revision received Dec. 11, 1998; accepted for publication Dec. 15, 1998. This paper is declared a work of the U.S. Government and is not subject to copyright protection in the United States.

*Research Aerospace Engineer, AFRL/VAAC, 2645 Fifth Street, Suite 7. E-mail: josyule@vaa.wpafb.af.mil.

†Research Aerospace Engineer, AFRL/VAAC, 2645 Fifth Street, Suite 7.